Role of the continuum background for carrier relaxation in InAs quantum dots

E. W. Bogaart,* J. E. M. Haverkort, T. Mano, T. van Lippen, R. Nötzel, and J. H. Wolter
COBRA Inter-University Research Institute, Department of Applied Physics, Eindhoven University of Technology, P.O. Box 513, 5600 MB Eindhoven, The Netherlands

(Received 24 November 2004; revised manuscript received 26 July 2005; published 1 November 2005)

We study the carrier capture and relaxation in self-assembled InAs/GaAs quantum dots (QDs) using bleaching rise time measurements as a function of the excitation density, at 5, 77, and 293 K. We observe that the bleaching rise time and the carrier lifetime of the first excited state are longer than the bleaching rise time of the QD ground state, indicating that the excited state does not act as an intermediate state. For high excitation density, we observe a temperature-dependent plateau in the initial bleaching rise time, contradicting an Auger-scattering-based relaxation model. Both these experimental results point toward a relaxation through the continuum background, followed by a single LO-phonon emission toward the QD ground state. The relaxation through the continuum background is governed by Coulomb or acoustic phonon coupling between the continuum and the discrete QD energy levels.

DOI: 10.1103/PhysRevB.72.195301 PACS number(s): 78.67.Hc, 78.47.+p, 42.65.−k

INTRODUCTION

One of the fundamental aspects of semiconductor quantum dots (QDs) is the discrete spectrum of eigenstates, due to the three-dimensional confinement. In reality, this ideal-atom picture is not observed. The deviation from the ideal-atom picture arises when the photoluminescence excitation (PLE) spectrum from a single QD is studied, showing not only sharp luminescence lines of the lower-lying QD eigenstates but also a nonzero continuum background.[1–9] Toda *et al.*[1] first suggested that the presence of such a continuum has major consequences for the energy relaxation of excited carriers within QD nanostructures. In order to explain the nonzero background, and moreover the associated relaxation channel, many concepts are proposed. Toda *et al.*[1] initially associated the continuum to the tail of wetting layer (WL) defect states, to which the carriers can relax their excess energy. However, Sanguinetti *et al.*[10] showed that even without the presence of the WL, fast carrier relaxation into the QD energy ground state (GS) is possible with similar relaxation times as observed in Stranski-Krastanow- (SK-)grown QDs. More recently, Vasanelli *et al.*[11] explained the continuum background in the PLE spectrum by the existence of crossed transitions between the bound QD states and delocalized states associated with the WL or barrier layer, hence, ascribing the continuum background as due to an intrinsic property of QDs. In this paper, we will show that the continuum background is not only important for explaining the single-QD PLE spectrum,[6,7,9] but the continuum background is also of prime importance for explaining the carrier capture and relaxation dynamics in a QD.

As suggested first by Toda *et al.*,[1] carrier relaxation takes place through the continuum background followed by a single LO-phonon emission. However, it should be noted that relaxation through the continuum is impossible as long as we ascribe the continuum as being due to *indirect-in-real-space* transitions[11] between the localized QD state and the WL state, since these transitions are not providing a relaxation channel within the QD. Any carrier relaxation through this continuum requires an additional coupling between the continuum and the confined QD states, either by a carrier-carrier scattering or phonon-scattering-induced process. Therefore, the efficiency of the continuum as a carrier relaxation channel is determined by the coupling strength between the continuum and the discrete QD levels.

CONTINUUM RELAXATION MODEL

In this paper, we propose that the carrier capture and relaxation process takes place in two steps, as is illustrated in Fig. 1: (i) the carrier relaxes through the continuum with a relaxation time that is solely determined by the coupling strength between the localized QD states and this continuum; (ii) this initial relaxation process is continued by a single LO-phonon emission process in which the carriers finally relax toward the QD GS. From our experimental results, we

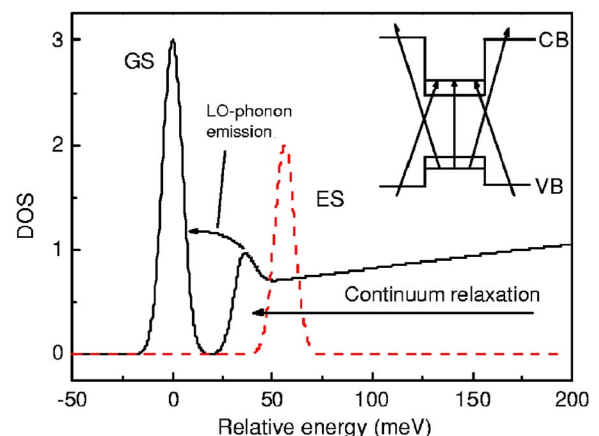

FIG. 1. (Color online) Schematic representation of the QD DOS, showing the continuum background which gives rise to a pathway for carrier relaxation. The LO-phonon replica is located near the onset of the continuum background, indicating that the carrier relaxation through the continuum is followed by a single LO phonon. The inset depicts the indirect-in-real-space transitions,[11] which give rise to the continuum background.

 ©2005 The American Physical Society

obtain several strong indications supporting this mechanism. First, at high excitation density, when Auger scattering is generally believed to be responsible for the carrier relaxation, our data show strong evidence that, apart from Auger scattering, a single LO-phonon emission process is still necessary in order to complete the total relaxation process. Second, within the usual relaxation picture, the uppermost confined QD energy levels are first occupied by carrier capture, followed by a carrier relaxation process within the QD in which the carrier relaxes down, passing the different exited states (ESs) toward the GS.[12] However, our results are in contradiction with this model, since we observe that the filling time as well as the carrier relaxation time of the first ES are longer than the filling time of the GS. This indicates that the carrier relaxes to the QD GS level without initially filling the excited states, thus pointing toward a relaxation through the continuum which initially bypasses the excited state.[11,13] The proposed relaxation channel through the continuum, is schematically illustrated in Fig. 1 showing the single LO-phonon line at the onset of the continuum background, in accordance with observed PLE spectra.[1,6,7]

Despite intensive investigations on the carrier capture and relaxation in QDs, the various explanations[1,10,11,14–18] for the relaxation channel which have been proposed do not provide a single coherent picture. In particular, a clear consensus for the detailed carrier relaxation mechanism is still lacking. To make an attempt to resolve this issue, we use two-color pump-probe time-resolved differential reflectivity (TRDR).[19,20] Using nonresonant excitation, carriers are excited within the barriers surrounding the QDs and diffuse from the barriers towards the QDs where they are captured and relax to the QD ground state. The probe beam monitors the absorption bleaching in the vicinity of the QD GS and ES transition. This experimental technique allows a direct comparison between the low temperature and room temperature carrier capture and relaxation. Moreover, TRDR is sensitive not only to the QD GS population, but also to populations of the excited states. The differential signal is directly related to the changes of the occupation of the QD eigenstates, i.e., $(R-R_0)/R_0=\Delta R/R_0 \sim (f_e+f_h)$, where f_e and f_h are the electron and hole occupation probabilities, respectively, whereas the photoluminescence (PL) signal is proportional to the product of the two probabilities, i.e., PL$\sim f_e f_h$. Therefore, by monitoring the occupation of the discrete QD energy states within the time domain, we are able to monitor the dominant mechanisms involved with the carrier relaxation processes. Finally, this technique allows us to simultaneously investigate the QD absorption spectrum, which is directly proportional to the QD density of states (DOS)[20] and is insensitive to the QD luminescence efficiency.

EXPERIMENTAL SETUP AND SAMPLE DETAILS

To determine the optical time response of the QDs, the sample is investigated by two-color time-resolved pump-probe differential reflection spectroscopy.[19,20] In this configuration, a 76 MHz mode-locked Ti:sapphire laser (Ti:S) is used as the pump source, and is mechanically chopped with a frequency of 4 kHz. The pump pulses are focused on the sample with a spot size of 55 μm, exciting carriers in the GaAs barrier layers in which they diffuse toward the QDs. The capture of the carriers into the QDs leads to bleaching of the QD transitions, and hence, a decrease of the probe pulse absorption and a change of the QD reflectivity. The pump-induced changes within the QD are probed by 200 fs and 2 ps pulses which are generated from an optical parametric oscillator. The probe pulse energy is tuned to the QD optical resonance, as is depicted in the inset of Fig. 2. The probe light is focused on the sample with a spot size of 25 μm using a graded index lens. Probe light reflected from the sample is collected by the same lens (so-called illumination and collection hybrid mode) and is focused on a balanced photodetector and subsequently measured by a lock-in amplifier to achieve a relative sensitively of 5×10^{-7}. The light collected by the detector is a superposition of the reflections of each layer, i.e., top surface, QD layers, and cross-product terms, as will be described below.

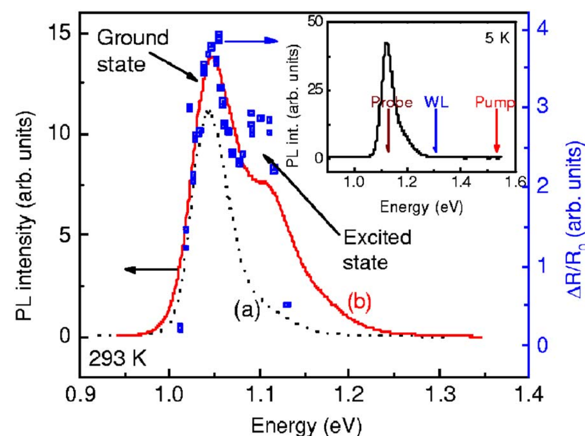

FIG. 2. (Color online) Room-temperature PL spectra of the QD sample for cw excitation (a), 250 mW/cm^2 at 2.33 eV, and pulsed excitation (b), 5 kW/cm^2 at 1.59 eV. The inset depicts the PL spectrum at 5 K (cw). The arrows indicate the photon energy of the pump and probe pulses and the energetic onset of the WL. The TRDR spectrum, i.e., the absorption bleaching spectrum, obtained at 293 K (squares) shows the GS as well as the first ES of the QD ensemble.

The time-resolved bleaching measurements are performed on a five-layer self-assembled InAs/GaAs QD sample grown by molecular beam epitaxy on GaAs (100), by the SK growth mode. After the deposition of a 295 nm GaAs buffer layer at 580 °C, the temperature was lowered to 490 °C for the growth of the multiple QD layers. A 30 nm GaAs layer was deposited before the growth of the five layers of QDs: 2.1 monolayers (ML) of InAs followed by 30 nm GaAs. Hereby, the QD layers can be considered as electronically uncoupled. Finally, the sample is capped by 137 nm GaAs at a temperature of 580 °C. Atomic force microscopy images show that the QDs are formed with a density of approximately 2.8×10^{10} cm^{-2}.

DIFFERENTIAL REFLECTIVITY OF QD STRUCTURES

In order to describe the reflection signal, we use a procedure similar to that of Tassone *et al.*[21] Although this method

was primarily developed to describe the response of quantum well systems, we assume that the model is also suitable for the description of the reflection response of QD structures. The QD size is small compared to the probe wavelength, such that the QDs are assumed to be electronically small.[22] Hence, the QD layer can be approximated by a thin layer with an average refractive index n_{QD}. The total reflection of the QD structure, taking into account all interferences between individual QD-layer and surface reflections, can be calculated analytically, in analogy with Ref. 21, in which case we obtain

$$|r_{tot}|^2 = \left| r_s + r_{QD} \sum_k \frac{C_k e^{i\phi_k}}{1 - C_k r_s r_{QD} e^{i\phi_k}} \right|^2, \tag{1}$$

where r_s and r_{QD} denote the sample surface and the QD-layer reflectivity, respectively. The summation takes into account the contribution of each QD layer, with C_k a correction term for the incident intensity, i.e., approximately $(1-r_s^2)$, and ϕ_k a phase difference induced by the total barrier width. Taking into consideration a homogeneous QD size distribution with a resonance frequency ω_0, which is broadened by radiative and nonradiative linewidths Γ and γ, respectively, Eq. (1) can be expressed by[21,23–25]

$$\begin{aligned} |r_{tot}|^2 &\simeq r_s^2 - 2(1 - r_s^2) r_s \\ &\quad \times \sum_k \left(\frac{(\Gamma + \gamma)\cos\phi_k + (\omega_0 - \omega)\sin\phi_k}{(\omega - \omega_0)^2 + (\Gamma + \gamma)^2} \right) \Gamma \\ &= R_s(\omega) + R_{QD}(\omega), \end{aligned} \tag{2}$$

where R_s is the constant surface reflection and R_{QD} can be written as $R_{QD}(\omega) = \mathcal{L}(\omega)\Gamma$, by introducing a line shape factor $\mathcal{L}(\omega)$.

Within the experiment, the photon energy of the probe light is far below the GaAs band gap, such that the pump-induced change of the GaAs refractive index within the probe energy window can be neglected.[26,27] The carrier-induced change in the QD reflectivity, that is, $(\partial/\partial\eta) R_{QD}(\omega) = \Delta R_{QD}(\omega)$, arises from the change in the QD oscillator strength[23,24] due to carrier capture, and hence a carrier-induced change of the radiative broadening. Thus, the pump-induced reflection change within the probe energy window is written as

$$\frac{\partial}{\partial\eta} R_{tot}(\omega) = \frac{\partial}{\partial\eta} R_{QD}(\omega) = \frac{\partial\Gamma}{\partial\eta} \frac{\partial}{\partial\Gamma} [\mathcal{L}(\omega)\Gamma(\omega)], \tag{3}$$

which can be rewritten as

$$\begin{aligned} \frac{\partial}{\partial\eta} R_{tot}(\omega) = \Delta R(\omega) &= \frac{\partial\Gamma}{\partial\eta} \left(\Gamma(\omega) \frac{\partial}{\partial\Gamma} \mathcal{L}(\omega) + \mathcal{L}(\omega) \frac{\partial}{\partial\Gamma} \Gamma(\omega) \right) \\ &= \Delta\Gamma[\Gamma(\omega)\mathcal{L}'(\omega) + \mathcal{L}(\omega)], \end{aligned} \tag{4}$$

with $\Delta\Gamma = \partial\Gamma/\partial\eta$. As is denoted by Eq. (4), the reflection spectrum includes the line shape factor $\mathcal{L}(\omega)$ and its derivative. In general $\Gamma \ll \omega_0$, which means that $|\mathcal{L}(\omega)| \ll |\mathcal{L}'(\omega)|$. Hereby, the differential reflection signal is expressed within the first-order approximation by

$$\frac{\Delta R(\omega)}{R_{tot}(\omega)} = \frac{R(\omega) - R_{tot}(\omega)}{R_{tot}(\omega)} \simeq \frac{\Delta R_{QD}(\omega)}{R_{tot}(\omega)} = \frac{\Delta\Gamma(\omega)\Gamma(\omega)\mathcal{L}'(\omega)}{R_{tot}(\omega)}. \tag{5}$$

The amplitude and the shape of the differential reflection signal depend on the QD sample structure through $\mathcal{L}'(\omega)$, which takes mutual interferences of the reflection signals of the QD layers into account. However, in Eq. (5) only the relative phase of the reflections is of importance. Due the symmetrical configuration with respect to the central QD layer, the odd parts of $\mathcal{L}'(\omega)$, i.e., $\sin\phi_k$, will cancel. Hence, the differential reflection signal has a typical Lorentzian behavior with a linewidth given by the radiative broadening Γ plus the nonradiative broadening γ. For real QD structures, however, due to the QD size distribution a summation over all homogeneous broadened QD states has to taken into account, which results in an inhomogeneous broadened QD DOS of the ensemble $[D(\omega)]$, such that $\mathcal{L}'(\omega) \to D(\omega)$. Hereby, the inhomogeneous broadened TRDR spectrum not only depicts the QD absorption spectrum, but also directly mirrors the DOS of the QD ensemble.

EXPERIMENTAL RESULTS AND ANALYSIS

PL and TRDR spectra

Figure 2 depicts the PL spectra of the QD ensemble at 5 and 293 K. For the excitation a cw neodymium-doped yttrium aluminum garnet (Nd:YAG) laser is used with an excitation density of 250 mW/cm^2 at a photon energy of 2.33 eV. Both spectra show a broadened main peak and a shoulder at the higher-energy side of the spectrum. The spectrum obtained at 293 K can be well deconvoluted using Gaussian functions with the main peak at an energy of 1.045 eV and with a width of 41 meV. However, the result of the deconvolution is not included in the figure for clarity. Using a mode-locked Ti:S laser (5 kW/cm^2 at 1.59 eV) as the excitation source, the first excited state is well observed in the spectrum *b* in Fig. 2. The excited state has a peak energy that is shifted over 56 meV with respect to the QD GS and has a width of 58 meV. Furthermore, the WL transition is located 168 meV above the QD GS, as is illustrated in the inset of Fig. 2. The measured TRDR curves, which are, e.g., shown in Fig. 3(a), are characterized by a rising edge governed by the capture and relaxation times as well as a decay. In addition, information about the QD absorption strength at the probe wavelength is contained in the amplitude of the $\Delta R/R_0$ signal. The solid points in Fig. 2 are the maxima of the TRDR signal for different probe wavelengths and thus represent the QD absorption bleaching spectrum. Figure 2 clearly shows both the GS and ES of the quantum dot, which emphasizes that the population dynamics of the GS as well as of the ES can be individually probed. For probe energies below 1 eV, no bleaching signal is observed. Deconvoluting the absorption spectrum by using two Gaussian functions provides two peaks with energies of 1.047 and 1.101 eV and with widths of 41 and 33 meV for the ground and excited state, respectively. It is observed that the GS spectra, i.e., from PL and TRDR, are well consistent con-

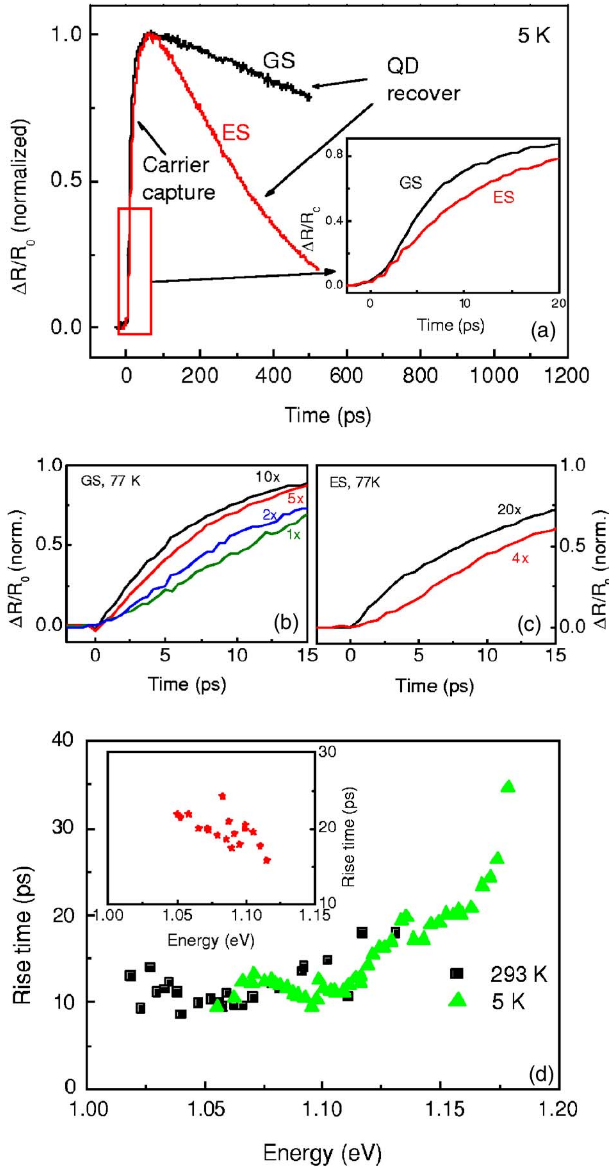

FIG. 3. (Color online) (a) Time evolution of the differential reflectivity signal of the QD GS and ES. The initial rise of the bleaching signal has a characteristic time of $\tau_{rise}=11.5$ and 24.4 ps for the GS and ES, respectively. The decay of the signal has a characteristic time of $\tau_{decay}=1708$ and 290 ps for the GS and ES, respectively. (b) and (c) Onset of the QD bleaching for different excitation densities, in units of $I_0=100\ \mathrm{W/cm^2}$, for the QD GS and ES, respectively. (d) Initial rise time as function of QD transition energy at 5 and 293 K for an excitation density of $200\ \mathrm{W/cm^2}$. The inset depicts the initial rise time at 77 K for an excitation density of $100\ \mathrm{W/cm^2}$.

cerning both the peak position and the width. The QD ES peak energy has a similar shift from the GS peak energy in both PL and TRDR. We would like to remark that similar results have been observed in our other samples with various configurations and materials composites, e.g., Refs. 20 and 28. In addition, within the spectral resolution of our measurements, we do not observe a Stokes shift between the absorption and the luminescence spectra.

In order to study the confinement of the carriers in the InAs QDs, temperature-dependent PL measurements are preformed between 5 and 293 K (not shown here). The integrated PL intensity is maintained up to 130 K and decreases exponentially with the increase of the temperature due to thermal quenching.[29,30] From the PL quenching, using an Arrhenius plot of $\ln(\int I_{pl})$ versus T^{-1}, an activation energy of 171 meV is deduced, which is consistent with the energy difference between the QD GS and the WL. Hence, a hole-confinement energy of 30–40 meV is deduced,[31] which indicates that the onset of the continuum background originates from the transition between the WL valence band continuum and the GS electron confinement state.[11] Moreover, the onset of the continuum is located in the vicinity of the first LO-phonon energy above the QD GS energy, as is illustrated in Fig. 1.

Carrier capture and relaxation

Energy dependence

The time evolution of the differential reflection signal of the GS and the first ES obtained at 5 K is presented in Fig. 3(a). The rise time of the bleaching signal is generally the overall carrier capture time of the probed QD energy level. The bleaching signal reaches its maximum value after a few picoseconds followed by an exponential decay, which directly monitors the carrier lifetime within the QD eigenstate. The bleaching time evolution can be described by

$$\frac{\Delta R}{R_0}(t) \sim [\exp(-t/\tau_{decay}) - \exp(-t/\tau_{rise})], \qquad (6)$$

with τ_{rise} and τ_{decay} the bleaching rise time and decay time, respectively. The filling of the quantum dot ES with a rise time of $\tau_{rise}=24.4\pm0.3$ ps is significantly longer than the GS rise time $\tau_{rise}=11.5\pm0.2$ ps, which means that the ES is being filled at a lower rate than the GS. Also, the decay of the excited state bleaching is much longer, $\tau_{decay}=290\pm2$ ps, than the rise time of the GS bleaching signal, indicating that the filling of the GS is not due to carrier relaxation from the first ES. The zero-time delay point is extrapolated from the experimental results. We want to emphasize that the rise time as is shown in Fig. 3, is in all measurements equal to the *initial* rise time of the differential signal, as is stressed by the enlargement in Fig. 3(a). To further emphasize that the observed excited state rise time is not determined by state filling, the onset of the QD bleaching is depicted in Figs. 3(b) and 3(c) for various excitation densities. We want to stress that for the initial rise times, state filling can by definition still be completely ignored. Since we measure the initial rise time, the relative long rise time of the excited state can not be due to state filling of the GS and subsequent filling of the ES. If we look to the rise time only, our result implies that the QD lowest energy level is being filled through a channel which circumvents the excited states. This mechanism is in contradiction with the idea of carrier relaxation within a QD starting at the highest confined QD level with a subsequent relaxation passing all other confined levels one by one.[12] On the other hand, this observation supports our idea that the

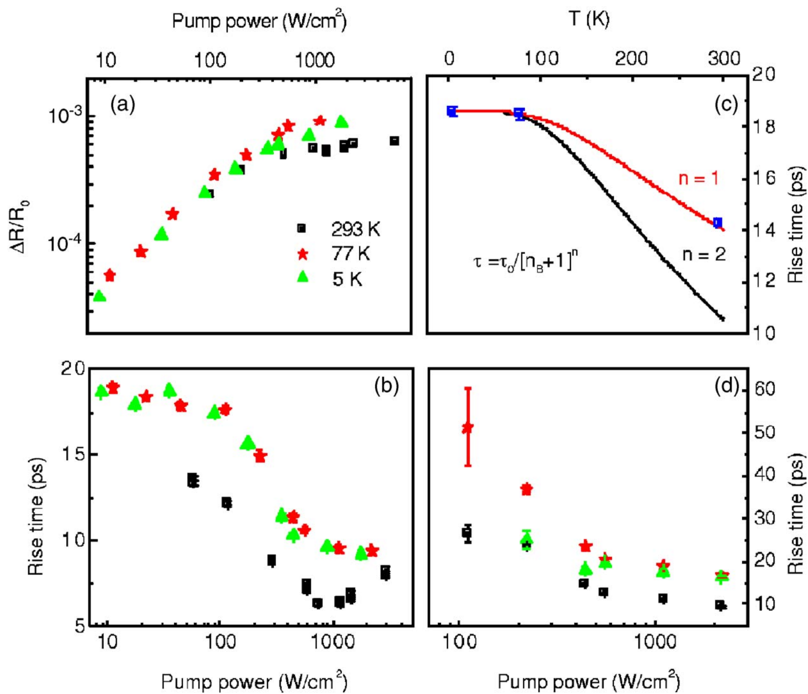

FIG. 4. (Color online) Amplitude of the QD bleaching (a) and the bleaching rise time (b) as functions of excitation power at 5 (triangles), 77 (stars), and 293 K (squares). (c) Bleaching rise time as a function of temperature for low excitation power. The fits represent the carrier relaxation by phonon emission for $n=1,2$, one phonon and two phonons, respectively. (d) Rise time of the bleaching signal of the first ES as a function of excitation power for various temperatures.

carriers relax through the continuum, continued by relaxation to the GS by single LO-phonon emission. In the latter picture, the ES rise time can be longer than the GS rise time when the coupling of the ES with the continuum is weak as compared to the coupling between the QD GS and the continuum. Finally, we note that if the occupation of the QD GS was due to carrier replenishment from higher-energy QD states, the time evolution of the GS occupation would show a plateaulike behavior before the exponential decay. This is not observed. These results more strongly suggest, that carriers captured in the excited energy states, are not responsible for the initial GS bleaching.

Figure 3(d) depicts an overview of the initial rise time as function of transition energy for various temperatures. A pronounced energy dependence is observed at $T=5$ K. Moreover, the observed increase of the rise time when tuning from the GS absorption peak toward the ES absorption peak, substantiates the long ES rise time as compared to the GS rise time.

Excitation density dependence

In order to reveal the underlying relaxation mechanism and to separate the effect of carrier-phonon and carrier-carrier scattering in the capture process, we analyze the bleaching rise time as a function of the pump excitation density. Figure 4(a) depicts the excitation dependence of the bleaching amplitude at the center of the GS transition, for various temperatures. For low excitation densities (<100 W/cm^2) the amplitude of the differential reflection signal increases linearly with increasing excitation, for all temperatures. In this regime, an average occupation density of less than one electron or hole per dot is assumed. For higher densities the signal deviates from the linear behavior, hence, the increase of the number of carriers per dot, and approaches an asymptotic value for excitation densities above 1 kW/cm^2. We would like to remark that the bleaching amplitude has decreased only by a factor of 2 by increasing the temperature from 5 up to 293 K.

Time-resolved measurements performed with different excitation powers show that the carrier capture and relaxation process strongly depends on the excitation density, as is depicted in Figs. 3(b) and 4(b). For low excitation densities (<100 W/cm^2) a near-constant initial rise time of about 20 ps is measured at 5 and 77 K. As the excitation density increases, the bleaching rise time decreases and approaches an asymptotic value of about 9 ps (>1 kW/cm^2). A similar behavior is observed for the bleaching rise time at 293 K, with a minimum value of 7 ps. The rise time values decrease with a $1/P$ dependence, with P the excitation density, which is common for a two-particle scattering process.[10,32] From these measurements it is clear, that the carrier capture process is dominated by different mechanisms for the two density regimes. The results as depicted in Fig. 4(b), are usually interpreted as being governed by phonon emission processes and by Auger scattering for low and high excitation densities, respectively.[16] The plateau value, which is reached for a density of approximately 1 kW/cm^2, has also been observed by other groups,[16,32] and is most easily interpreted as being due to state filling, but we will argue below that this can not be the case for our measurements. First, the observed temperature dependence of the plateau value can not be explained by the state-filling argument. Second, as we have previously indicated, the initial rise time can impossibly be influenced by state filling. Finally, if the plateau value were due to state filling, we would expect a fast initial rise followed by saturation of the bleaching signal which has not been observed.

Due to the excitation within the GaAs barriers, the carriers have to diffuse toward the QDs in order to be captured. This means that the rise time of the bleaching signal is also affected by the carrier diffusion time and the local capture

time. Hence, the plateau at high carrier density might be governed by these two processes. However, the carrier capture process within the continuum is assumed to be fast,[2,32] <1 ps, and the carrier diffusion decreases with increasing temperature,[33–35] which is in contradiction with the temperature dependence of the high carrier density plateau, as is depicted in Fig. 4(b). Therefore, we believe that the bleaching of the QD energy transitions is dominated by the intradot energy relaxation.

In our model, the plateau for low excitation densities, below 100 W/cm^2, is interpreted as being due to relaxation through the continuum, which is only weakly coupled to the QD eigenstates by most probably LA phonons, continued by a single LO-phonon emission. With the increase of the pump-induced carrier density, Auger scattering becomes more important and directly contributes to the relaxation process. However, carrier relaxation in which the Auger process becomes the dominant carrier relaxation mechanism, is not in accordance with our measurements, since the data still show a significant temperature dependence, as is depicted in Fig. 4(b). In the continuum relaxation model, Auger scattering is one of the possible mechanisms that will increase the coupling between the continuum and the confined QD energy levels, thus facilitating the relaxation through the continuum. It should, however, be pointed out that other carrier-carrier scattering mechanisms such as electron-hole (*e*-*h*) scattering[36,37] within the QD will also be enhanced for higher excitation densities. Unfortunately, we have to remark that, although TRDR is sensitive to the individual occupation dynamics of the electron and hole levels separately, f_e and f_h, respectively, we have not observed an initial rapid increase of the bleaching signal due to the fast hole relaxation, followed by a second bleaching signal due to *e*-*h* scattering[36,37] throughout the whole measurement series. In our model, we do not claim that we can separate the effects of Auger scattering and *e*-*h* scattering, but we only emphasize that both these mechanisms are likely to enhance the continuum relaxation both directly and by coupling the continuum with the QD levels.

Finally, for excitation densities above 1 kW/cm^2, the Auger-mediated relaxation through the continuum is very fast, leaving the final single LO-phonon emission process as the limiting step in the relaxation path, which is believed to be responsible for the observed plateau for high excitation density. Moreover, for high densities the bleaching rise time is equivalent to the LO-phonon lifetime in GaAs, i.e., 5–10 ps,[32,38] which suggests that the final optical phonon emission process is limited by the hot-phonon effect. This result endorses our idea that the final step in the relaxation path through the continuum involves a single LO-phonon emission, as is illustrated in Fig. 1.

Further evidence for our model is provided by Fig. 4(c), where we plot the temperature dependence of the bleaching rise time for low excitation density. The temperature dependence can be fitted by assuming that the carrier relaxation is governed by the emission of one or multiple LO phonons, $\tau=\tau_0/[n_B+1]^n$,[16,39] as is depicted in Fig. 4(c). In this equation, n_B is the Bose-Einstein distribution function for LO phonons, and n takes into account the number of LO phonons which are emitted during the relaxation process. For the calculation we have used the GaAs LO-phonon energy. The temperature dependence, as is shown in Fig. 4(c), clearly indicates that the carrier capture and relaxation process in a QD at least includes the emission of a single LO-phonon process, i.e., the best fit is obtained for $n=1$, consistent with the previous results and with our continuum relaxation model.

Finally, we have measured the bleaching rise time of the first excited QD eigenstate as function of the pump excitation power for various temperatures, as is depicted in Fig. 4(d). The observed dependence on the excitation density and temperature is similar as in the case of the GS bleaching rise time, indicating that our results are mutually consistent. Moreover, the ES rise times are consistently longer than the GS rise times for all temperatures and excitation densities. The relatively long rise time of the ES with respect to the GS indicates that the ES is not acting as an intermediate level in the carrier relaxation process toward the QD GS.

Since the measured continuum background in PLE usually extends down to a single LO-phonon energy above the QD ground-state energy,[1,6–8] and the ground-excited state energy splitting is 56 meV, the continuum overlaps with the excited state transitions. This disputes the idea of isolated excited-states, as is schematically illustrated in Fig. 1. In addition, from the carrier confinement energy (171 meV) a hole-confinement energy of 30–40 meV is deduced. This indicates that the onset of the continuum arises from the transition between the WL valence band continuum and the first electron confinement state,[11] located in the vicinity of the first LO-phonon energy above the QD GS energy. Surprisingly, the coupling of the continuum with the ES is weaker than the coupling with the GS, as is evidenced from the relative long rise time for the first excited state. A possible explanation for the different coupling is as follows: The continuum is, according to Ref. 11, formed by indirect-in-real-space transitions between the QD ground state and the WL, and hence is connected to the GS transition. In the absorption, the ES gives rise to its own continuum, which consists of indirect-in-real-space transitions between the QD excited state and the WL. The onset of the continuum associated with the ES arises from the transition between the WL valence band continuum and the first excited electron state within the QD. The efficiency of the coupling strength of a continuum associated with the excited state is expected to be lower due to the odd symmetry of the ES envelope wave function. Hence, it is expected that the carrier relaxation occurs in the continuum associated with the QD ground state, and with the final relaxation down to the ground state by LO-phonon emission.

SUMMARY

In summary, carrier capture and relaxation processes of self-assembled InAs/GaAs QDs have been studied directly, by means of two-color TRDR for various temperatures and pump excitation densities. Fast carrier capture and relaxation is observed. The initial bleaching rise time and the carrier relaxation time of the first ES are longer than the initial rise time of the QD GS, indicating that the excited state does not

act as an intermediate state. A temperature-dependent plateau in the initial bleaching rise time is observed at high excitation density, contradicting a relaxation model based purely on Auger scattering. Both these experimental results point toward a relaxation through the continuum background, followed by a single LO-phonon emission toward the QD ground state. Finally, we would like to remark that the proposed mechanism of continuum relaxation followed by a single LO-phonon emission might provide a basis for integrating the various explanations of previous experiments, considering phonon-mediated relaxation and Coulomb scattering.

ACKNOWLEDGMENTS

We sincerely acknowledge J. M. van Ruyven for technical support. This work is financially supported by the Dutch Foundation for Research on Matter (FOM).

*Electronic address: e.w.bogaart@tue.nl

[1] Y. Toda, O. Moriwaki, M. Nishioka, and Y. Arakawa, Phys. Rev. Lett. **82**, 4114 (1999).
[2] R. Heitz, M. Veit, N. N. Ledentsov, A. Hoffmann, D. Bimberg, V. M. Ustinov, P. S. Kop'ev, and Z. I. Alferov, Phys. Rev. B **56**, 10435 (1997).
[3] C. Kammerer, G. Cassabois, C. Voisin, C. Delalande, P. Roussignol, and J. M. Gérard, Phys. Rev. Lett. **87**, 207401 (2001).
[4] L. Besombes, J. J. Baumberg, and J. Motohisa, Phys. Rev. Lett. **90**, 257402 (2003).
[5] M. J. Steer, D. J. Mowbray, W. R. Tribe, M. S. Skolnick, M. D. Sturge, M. Hopkinson, A. G. Cullis, C. R. Whitehouse, and R. Murray, Phys. Rev. B **54**, 17738 (1996).
[6] F. Findeis, A. Zrenner, G. Böhm, and G. Abstreiter, Phys. Rev. B **61**, R10579 (2000).
[7] A. Lemaître, A. D. Ashmore, J. J. Finley, D. J. Mowbray, M. S. Skolnick, M. Hopkinson, and T. F. Krauss, Phys. Rev. B **63**, 161309(R) (2001).
[8] J. J. Finley, A. D. Ashmore, A. Lemaître, D. J. Mowbray, M. S. Skolnick, I. E. Itskevich, P. A. Maksym, M. Hopkinson, and T. F. Krauss, Phys. Rev. B **63**, 073307 (2001).
[9] R. Oulton, J. J. Finley, A. I. Tartakovskii, D. J. Mowbray, M. S. Skolnick, M. Hopkinson, A. Vasanelli, R. Ferreira, and G. Bastard, Phys. Rev. B **68**, 235301 (2003).
[10] S. Sanguinetti, K. Watanabe, T. Tateno, M. Wakaki, N. Koguchi, T. Kuroda, F. Minami, and M. Gurioli, Appl. Phys. Lett. **81**, 613 (2002).
[11] A. Vasanelli, R. Ferreira, and G. Bastard, Phys. Rev. Lett. **89**, 216804 (2002).
[12] J. Urayama, T. B. Norris, J. Singh, and P. Bhattacharya, Phys. Rev. Lett. **86**, 4930 (2001).
[13] B. Urbaszek, E. J. McGhee, M. Kruger, R. J. Warburton, K. Karrai, T. Amand, B. D. Gerardot, P. M. Petroff, and J. M. Garcia, Phys. Rev. B **69**, 035304 (2004).
[14] U. Bockelmann and T. Egeler, Phys. Rev. B **46**, 15574 (1992).
[15] T. Inoshita and H. Sakaki, Phys. Rev. B **46**, R7260 (1992).
[16] B. Ohnesorge, M. Albrecht, J. Oshinowo, A. Forchel, and Y. Arakawa, Phys. Rev. B **54**, 11532 (1996).
[17] H. Htoon, D. Kulik, O. Baklenov, A. L. Holmes, T. Takagahara, and C. K. Shih, Phys. Rev. B **63**, 241303(R) (2001).
[18] S. Marcinkevičius and R. Leon, Phys. Rev. B **59**, 4630 (1999).
[19] A. Othonos, J. Appl. Phys. **83**, 1789 (1998).
[20] E. W. Bogaart, J. E. M. Haverkort, T. Mano, R. Nötzel, J. H. Wolter, P. Lever, H. H. Tan, and C. Jagadish, IEEE Trans. Nanotechnol. **3**, 348 (2004).
[21] F. Tassone, F. Bassani, and L. C. Andreani, Phys. Rev. B **45**, 6023 (1992).
[22] G. Y. Slepyan, S. A. Maksimenko, V. P. Kalosha, A. Hoffmann, and D. Bimberg, Phys. Rev. B **64**, 125326 (2001).
[23] F. Fernández-Alonso, M. Righini, A. Franco, and S. Selci, Phys. Rev. B **67**, 165328 (2003).
[24] L. C. Andreani, G. Panzarini, A. V. Kavokin, and M. R. Vladimirova, Phys. Rev. B **57**, 4670 (1998).
[25] O. Stefano, S. Savasta, and R. Girlanda, Phys. Rev. A **60**, 1614 (1999).
[26] J. Shah, *Ultrafast Spectroscopy of Semiconductors and Semiconductor Nanostructures* (Springer, Berlin, 1996).
[27] J. P. Callan, A. M. T. Kim, C. A. D. Roeser, and E. Mazur, in *Ultrafast Physical Processes in Semiconductors* (Academic Press, New York, 2001).
[28] E. W. Bogaart, R. Nötzel, Q. Gong, J. E. M. Haverkort, and J. H. Wolter, Appl. Phys. Lett. **86**, 173109 (2005).
[29] G. Bacher, H. Schweizer, J. Kovac, A. Forchel, H. Nickel, W. Schlapp, and R. Lösch, Phys. Rev. B **43**, R9312 (1991).
[30] R. Leon, Y. Kim, C. Jagadish, M. Gal, J. Zou, and D. J. H. Cockayne, Appl. Phys. Lett. **69**, 1888 (1996).
[31] S. J. Sun and Y.-C. Chang, Phys. Rev. B **62**, 13631 (2000).
[32] D. Morris, N. Perret, and S. Fafard, Appl. Phys. Lett. **75**, 3593 (1999).
[33] *Physics of Group IV Elements and III-V Compounds*, edited by K. H. Hellwege, New Series, Group III, Landolt-Börnstein, Vol. 17 (Springer-Verlag, Berlin, 1982).
[34] M. Neuberger, *III-V Semiconductor Compounds*, Handbook of Electronic Materials Vol. 2 (IFI/Plenum, New York, 1971).
[35] J. F. Young and H. M. van Driel, Phys. Rev. B **26**, 2147 (1982).
[36] H. Jiang and J. Singh, Physica E (Amsterdam) **2**, 720 (1998).
[37] T. S. Sosnowski, T. B. Norris, H. Jiang, J. Singh, K. Kamath, and P. Bhattacharya, Phys. Rev. B **57**, R9423 (1998).
[38] S. D. Sarma, *Hot Carriers in Semiconductor Nanostructures* (Academic Press, London, 1992).
[39] M. D. Giorgi, C. Lingk, G. von Plessen, J. Feldmann, S. D. Rinaldis, A. Passaseo, M. D. Vittorio, R. Cingolani, and M. Lomascolo, Appl. Phys. Lett. **79**, 3968 (2001).